Eur. Phys. J. Plus (2022) 137:430
https://doi.org/10.1140/epjp/s13360-022-02605-x

THE EUROPEAN PHYSICAL JOURNAL PLUS

Regular Article

Multiscale roughness analysis by microprofilometry based on conoscopic holography: a new tool for treatment monitoring in highly reflective metal artworks

Claudia Daffara[1,a], **Sara Mazzocato**[1], **Giacomo Marchioro**[2]

[1] Department of Computer Science, University of Verona, Strada le Grazie 15, 37134 Verona, Italy
[2] Department of Cultures and Civilisations, University of Verona, v.le dell'Università 4, 37129 Verona, Italy

Received: 24 September 2021 / Accepted: 15 March 2022

Abstract The analysis of surface roughness in highly reflective metal artworks is challenging and requires contactless devices capable to measure regions with high micrometer accuracy in both depth and lateral directions. We demonstrate optical profilometry based on scanning conoscopic holography for micrometer measurement of silver samples treated with different hand-made cleaning processes. The technique is shown effective in acquiring shiny and smooth metal samples providing high-resolution and high-accurate dataset (0.1 μm depth and 5 μm lateral resolution) that is a reliable representation of the microsurface structure. From a statistical point of view, the cleaning treatments have the same nature of the low-abrasion, but the underlying mechanical processes are different. This fact suggested a more in-depth study of both the amplitude and the hybrid areal roughness parameters. It is proposed a workflow for a dual integrated multiscale roughness analysis for surface characterization: a scale inspection to detect possible texture non-homogeneity, and a signals separation to outline the most significant texture components. The scale-limited components allowed to discriminate the different surface processes. The results on silver samples demonstrate the potential of multiscale roughness analysis by conoscopic holography as a new tool for treatment monitoring in metal artworks.

1 Introduction

In this work, we present the potentialities of optical scanning microprofilometry based on conoscopic holography in the challenging measurement of highly reflective and smooth surfaces of artistic interest, such as those of artifacts of silver- and copper-based alloys. These materials are very sensitive to degradation phenomena in the interaction with the surrounding environment [1–3], such as corrosion due to atmosphere gases and humidity. The outcome of the corrosion processes is the alteration of the surface with formation of tarnishing, encrustations, and pits at micron scale, depending on the extent of corrosive phenomena. Degraded artworks require extensive conservation treatments for the removal of the alteration and the protection of the metal surface against further interactions. Best practice in Cultural Heritage applications requires quality control procedures to verify that artworks treatments are not only effective but also (ideally completely) noninvasive [4–7].

A review of nondestructive physical sensing methods to characterize the artwork condition and the cleaning process is given in [8]. Regarding the analysis of the microsurface morphology, optical coherence tomography (OCT) was shown effective for the profilometry of the topmost varnished semi-transparent layer and it is widely used in paintings [8–10], while laser scatterometry was used for sampling the opaque, highly smooth surface finishes of bronze materials [8]. This latter technique has small field of view (millimeters) and working range (from nanoscale to micron), it provides a measurement of the sub-micron surface roughness locally but it is not suitable for monitoring irregular surfaces in artwork treatments. Local changes of the microsurface in artwork treatments were monitored through an analysis of representative spots also using stylus-based roughness testers that provide a contact measurement of standard roughness parameters in a one-dimensional profile [11], or using optical surface analyzers able to acquire the 2D topography (area of size 25 mm^2) [12]. Such devices are compact and portable, but the use of stylus or probes in contact with the surface is not an optimal choice in Cultural Heritage, where a safe working distance is desirable also for optical probing. A topographical assessment of cleaning treatments based on amplitude roughness parameters on randomly selected areas was proposed using a benchtop profilometer based on white light interferometry [7]. Performance analysis of silver cleaning treatments is usually being carried out by inspecting the surface morphology on scanning electron microscopy (SEM) micrographs and atomic force microscopy (AFM) height maps [4–6,13]. Such techniques allow to inspect the surface texture up to the nanoscale, but they are limited to a small area of the sample and cannot operate in situ. As emphasized in the literature [4], manual procedures as mechanical cleaning are subjective and may produce non-homogeneous surface finishes.

[a] e-mail: claudia.daffara@univr.it (corresponding author)

Published online: 07 April 2022

In short, the potential of surface microprofilometry for artworks applications is recognized, taking advantage of the commercial availability of portable and benchtop instrumentation; the major limitations are still concerned with the need for portable devices that enable a non-contact measurement in whole-field.

To fulfill this requirement, optical scanning profilometry mounting conoscopic laser probes was introduced in early works [14] for acquiring the surface morphology in macro-regions (in the order of tens of centimeters) and estimating a global, averaged roughness.

Laser conoscopic holography is a non-contact and noninvasive technique [15] that provides an interferometric measurement of distances within a versatile working range maintaining a micrometric accuracy [16]. The potentiality of the technique was proved on different heritage applications, e.g., in archeology [14,17], as complementary analysis in painting conservation [18,19], up to the recent 3D printing of artworks for tactile fruition [20]. The state-of-the-art applications in the field do not report the use of the technique for monitoring the microsurface modifications in highly reflective metal artworks. Shiny surfaces are challenging for whole-field optical profilometry in general, but conoscopic holography has been shown to provide stable measurements [21,22]. However, a high depth and lateral resolution is required for sampling meaningful surface information in metals. The mentioned scanning profilometry, which was tailored to the diagnostics of diffusive objects such as bronzes [14] and paintings [18,19] with surface heights scaled in the order of tens and hundreds of microns, has a lateral resolution down to 20 μm mainly limited by the laser spot size.

Motivated by this framework, we propose the use of a customized microprofilometer based on scanning conoscopic holography and a multiscale roughness analysis as new tool for surface characterization in the treatments of highly reflective metal artworks. As proof of concept of the technique, silver surfaces subjected to different treatments were measured where, in particular, different mechanical cleaning procedures were tested. In addition to the importance of measuring locally the micron-scale roughness of smooth and shiny surfaces in metal objects, the other challenge was to have a technology that enabled the acquisition of macroscopic regions while maintaining high resolution: this allows to detect the modifications of the roughness globally, to supervise the non-homogeneity of the texture, and to map the contribution from single "defective" events.

2 Materials and methods

2.1 Conoscopic holography-based micron-scale profilometry

In order to effectively acquire the surface texture in silver artworks at micron scale and to sample meaningful roughness and waviness information, a microprofilometry technique with high-resolution capability in both depth (sub-micron) and lateral (micron) directions as well as with whole-field capability (tens of centimeters) is desirable. To this aim, we optimized an ad hoc, portable microfilometer using single-point, interferometric depth-sensors based on conoscopic holography and micrometric scanning method [21]. The object is scanned by the optical probe using a system of linear stages orthogonally mounted, the optical probe measures the depth distance in the line-of-sight direction orthogonal to the xy scanning grid. The motion system has 30 cm × 30 cm of maximum scan size, and a minimum incremental motion of 0.1 μm.

For acquiring the highly reflective surface of silver samples, it is employed the conoscopic sensor ConoPoint-3R (available from Optimet) that nominally reaches sub-micron depth resolution with lateral resolution down to the micron. The main advantage of the conoscopic holography sensors is the versatile measuring range, which can be tailored to the scale of the object using different lenses. High resolution (i.e., small laser spot size) is obtained at the cost of the working range (Table 1).

In this study, a 25 mm focal lens was used. The laser spot is less than 5 μm (FWHM size at standoff position) and it enables to perform high-resolution, micron-scale scanning profilometry for acquiring the roughness signal in silver samples. The downside of precision scanning is that it is time consuming, even with the sensor triggered for acquisition in continuous mode.

2.2 The proof of concept on silver cleaning treatment

The proof of concept of the high-resolution, conoscopic holography-based profilometer is given on a case study on the treatment of tarnished silver decorations provided by the Restoration Laboratories of the Opificio delle Pietre Dure, Institute of the Italian Ministry for Cultural Heritage. As alternative to the mechanical traditional methods based on abrasive powder dispersed in liquid,

Table 1 Nominal characteristics of the possible probe-lens couplings

Lens mm	Measurement range (mm)	Standoff (mm)	Accuracy* (μm)	Laser spot size(μm)	Angular coverage (°)
25	1	16	1	5	5
50	5	40	2.5	16	3
75	9	65	4.5	25	1.5

*Difference between two flat surfaces measured as compared to nominal value

Table 2 Main characteristics of the silver samples. Details can be found in [6]

Mockup symbol	Cleaning treatment	Abrasive medium	Grain size (μm)
Pw-A	Water suspension of Sodium hydrogen carbonate	Sodium bicarbonate	300–500
Pw-B	Water suspension of Calcium carbonate	Calcium carbonate	100
Pd-RC	Dry, with rubber, refill	Calcium carbonate	1–30
Pd-RD	Dry, with rubber, piece	Calcium carbonate	1–50
Pd-RE	Dry, with rubber, pencil	Calcium carbonate	1–35
Pd-DF	Dry, with dental rubber, wheel	Zirconium grain	1–10
Pd-DG	Dry, with dental rubber, pointed	Aluminum oxide grain	1–10

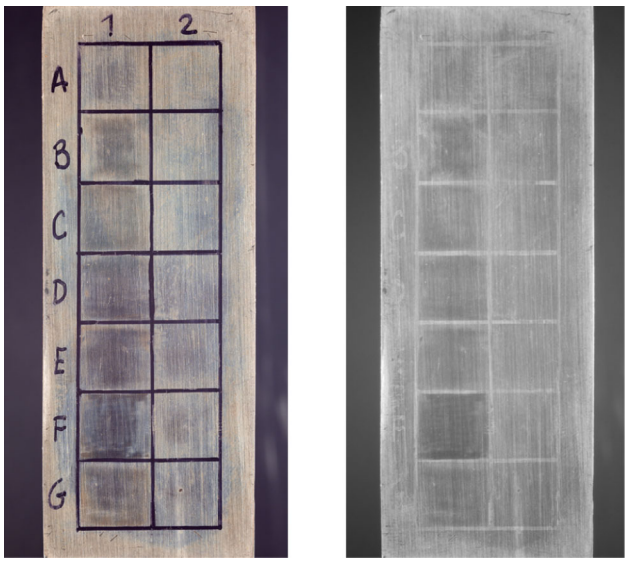

(a) VIS **(b)** NIR (950–1050 nm)

Fig. 1 Technical photography (CMOS camera) of the mockup. Letters refer to the treatments in Table 2; here, the column (2) has not been treated

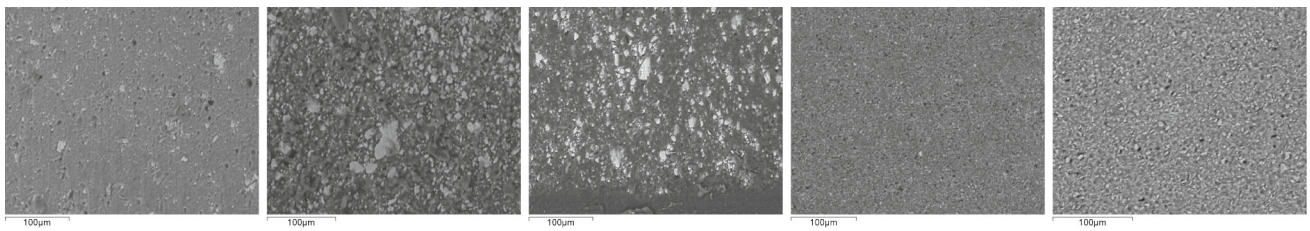

(a) Pd-RC **(b)** Pd-RD **(c)** Pd-RE **(d)** Pd-DF **(e)** Pd-DG

Fig. 2 Grain size of the abrasive rubbers observed with SEM; same scale of 100 μm

Basilissi [6] introduced an innovative dry-cleaning method based on erasers for restoring the Lorenzo Ghiberti's North Door of the Florence Baptistery. It was the occasion to test the microprofilometer as novel complementary technique for investigating the effects on the surface trough a quantitative roughness analysis, as the laboratory microscopy techniques used for inspecting surface morphology could only detect the single defect locally [6], without providing an objective measure of the micro-texture over the sample.

Microprofilometry was performed on exemplary mockups reproducing some mechanical cleaning treatments on silver, with the surface finished using different abrasive mediums: traditional wet methods with abrasive powder and the dry-cleaning methods that use rubbers as abrasive tools were considered (Table 2). In Fig. 1, technical photography in the visible (VIS) and in the near infrared (NIR) range of the silver mockup is reported. VIS-NIR photography allows to appreciate, in a qualitative way, some marks left by the treatments, for which a quantitative analysis is desirable.

The images taken on a SEM (Fig. 2) show the different sizes and distributions of the abrasive grains in the rubber-based cleaning tools.

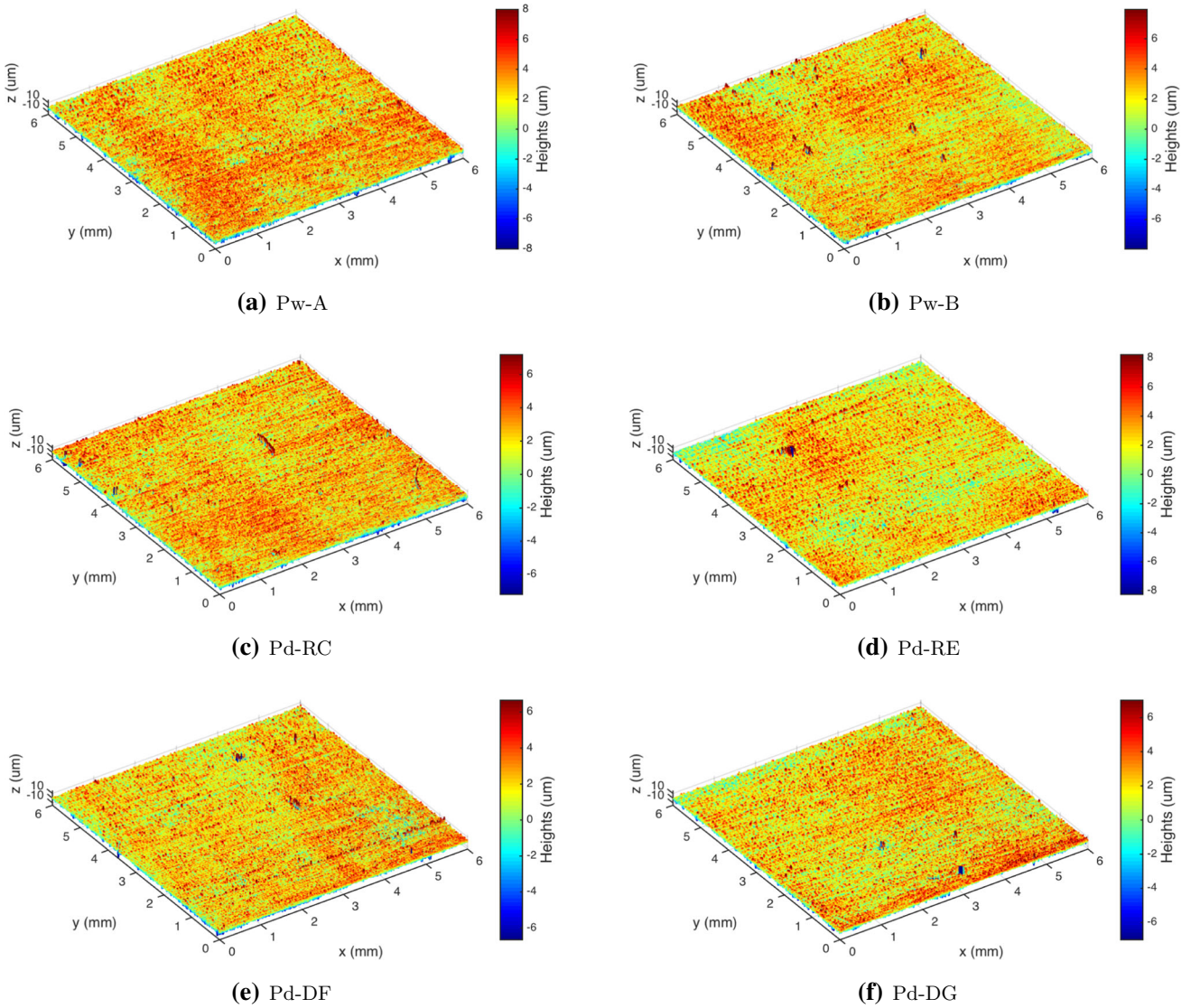

(a) Pw-A **(b)** Pw-B

(c) Pd-RC **(d)** Pd-RE

(e) Pd-DF **(f)** Pd-DG

Fig. 3 Surface texture of the samples (5 µm scan step), heights data visualized in a three-sigma range from the mean

2.3 The microprofilometry dataset

The samples were acquired with a 5 µm scanning step in both the x and y direction. The quality of the single-point measurement performed by the conoscopic holography sensor was controlled by providing a signal-to-noise ratio (SNR) greater than 50% and the correct working distance according to the lens-probe coupling. Figure 3 shows the three-dimensional topography maps obtained from the surface heights data acquired by the microprofilometer, on which it was carried out the multiscale roughness analysis described below. It is visually observable the non-uniformity of the surface finish, the surface lay, and some local defects (e.g., scratches, craters) in the silver samples.

Figure 4 shows a representative 1 mm^2 ROI for each silver sample that allows to appreciate the surface asperities at micron scale generated in the treatments.

In detail, the scan velocity was set at 5 mm/s along the main scanning x-axis and at 1.5 mm/s along the sub-scanning y-axis. The measured repeatability, i.e., the standard deviation of 10000 static measurements of the silver surface, was 0.1 µm.

During the analysis, it was decided to not consider the sample `Pd-RD` because the tool used was deemed too large compared to the size of the sample.

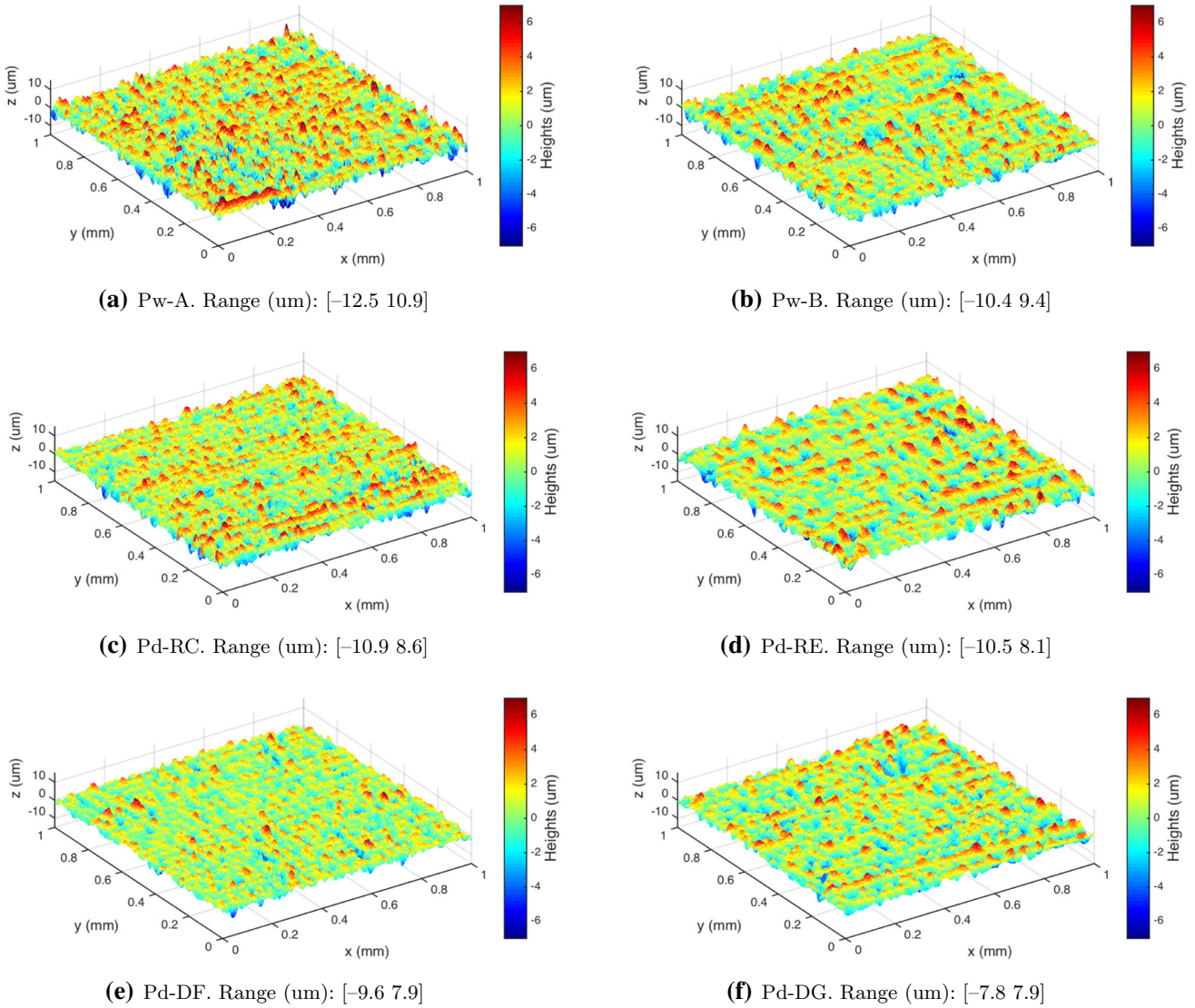

(a) Pw-A. Range (um): [–12.5 10.9]

(b) Pw-B. Range (um): [–10.4 9.4]

(c) Pd-RC. Range (um): [–10.9 8.6]

(d) Pd-RE. Range (um): [–10.5 8.1]

(e) Pd-DF. Range (um): [–9.6 7.9]

(f) Pd-DG. Range (um): [–7.8 7.9]

Fig. 4 Representative ROI of 1 mm^2 visualized in the same colormap and scale for comparison. The min–max range of each ROI is also provided

2.4 Multiscale analysis of surface data

A surface is a complex structure that includes several length scales (i.e., wavelengths) of superimposed roughness, which are then reproduced in the digitized surface according to the properties of the instrument, with the shortest spatial structure set by the sampling step and the longest one by the sampling length. The approach in surface metrology is to divide the surface signal in components of different bandwidths along the scan length [23]: after separating the texture from the shape, the roughness (irregularities at smaller scales) and the waviness (more widely spaced variations) are studied. The length scale characterizing the roughness and waviness signals should be chosen by relating these scale-limited features to the process in which they are generated. However, an ancient artwork is a unique piece that is not the result of an engineered process and, over time, it is exposed to events, such as material degradation and manual conservation treatments, which make its surface history complex and unknown.

From the dataset acquired on the silver samples (Figs. 3 and 4), it is shown that the profilometer is capable of detecting fine local defects and a micron-spaced roughness pattern with irregular waviness features over a macro (millimeter) spatial scale. Surface characterization was performed using a multiscale approach [24,25], by inspecting the variation of the roughness features with the scale. Preliminary testing of the multiscale analysis for diagnostics can be found in our previous work [26], while a general, integrated procedure was developed here. Further areal surface texture parameters from the international standards [27,28] were considered (see "Appendix" for the mathematical definition):

1. amplitude parameters, estimating the average behavior of the surface heights: root mean square (RMS) roughness (Sq), skewness (Ssk), kurtosis (Sku), and peak-to-valley roughness (Sz);

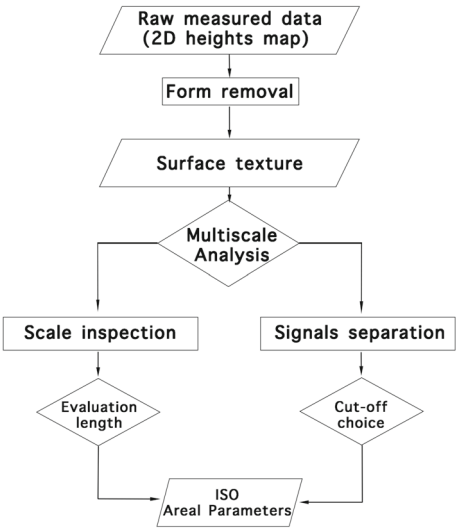

Fig. 5 Flowchart of the multiscale surface analysis based on scanning microprofilometry

2. hybrid parameters, combining height-lateral information: RMS gradient (Sdq), and developed interfacial area ratio (Sdr).

Surface data analysis follows the workflow depicted in Fig. 5. As first, the shape is removed from the measured data to obtain the texture signal. Then, in a new approach, two different kinds of multiscale analysis are carried out, in parallel.

Scale inspection: the scale-limited roughness parameters are studied with the variation of the evaluation length, by inspecting the sample in subregions.
Signal separation: the separation of roughness and waviness is performed on the whole sample by Gaussian filtering with different cutoff values, and the roughness parameters are studied in the scale-limited surface components.

3 Results

As a first analysis of the samples and the involved treatments, we explored the representation of the surface in function of combination of two selected parameters. It was decided to apply a five-sigma threshold on the dataset, as from the inspection of the heights maps it was the best value for filtering out some accidental defects of the silver plate (deeper scratches and craters, order of hundreds of microns) while accounting for the traces caused by the surface treatments (order of tens of microns).

Figure 6 (left) shows the coordinate system of Ssk and Sku. These two amplitude parameters are mathematically independent and they usually display a nearly parabolic behavior that tends to depend on machining process. As can be seen, all the samples are located in the same region, i.e., in the left half of the map with negative skewness, which indicates the same underlying finishing process. Figure 6 (right) shows the interrelation between the hybrid parameters Sdq and Sdr. As shown in literature [29], these parameters can have an interesting correlation. In this case, the interrelation between these parameters seems to be confirmed, except for the sample `Pd-DG`. The surfaces are clearly distinguishable in the plane, but all fall within the area where surfaces showing not oriented types of machining are usually found. Looking at the definitions (see "Appendix A"), it can be figured out that the Sdq-Sdr space carries information about the orientation of the surface: higher values of Sdq are expected in the case of a surface with slope in various directions.

3.1 Scale inspection

Following the flowchart in Fig. 5, this phase aimed to deeply study the surface using the multiscale approach for inspecting the variation of the roughness features with the observation scale, as the hand-made treatments could be non-homogeneous. In the previous preliminary work [26] it was observed that as the scan length enlarged, the roughness parameter Sq tended to stable values, indicating a long-wavelength stationary behavior in relation to the underlying process. Thus, we estimated the Sq roughness globally in the entire sample surface and locally in a representative ensemble constructed by running a fixed-size ROI.

We found that the silver surface processed by the rubbers and the one polished with abrasive powders have similar Sq roughness (Fig. 7). This result was used in the mentioned work by Basilissi [6] to support the validation of the dry-cleaning method as noninvasive surface treatment compatible with the traditional methods. The local roughness is generally not uniform, as shown from the boxplots of the distribution of the Sq computed in the ROIs and from the subsets map (Fig. 8). At the millimeter-scale, the coefficient of variation (σ/μ) varies from 0.04 to 0.11, with the higher value for the surface finished with the wheel tool (`Pd-DF`).

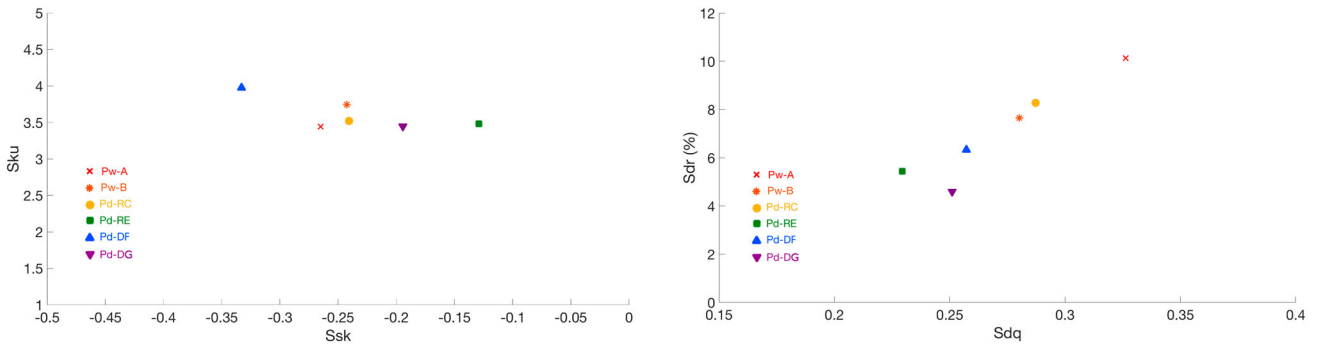

Fig. 6 Kurtosis (Sku) versus skewness (Ssk) and RMS gradient (Sdq) versus developed interfacial area ratio (Sdr) for the analyzed samples. The parameters are estimated globally in the entire samples

Fig. 7 Roughness of the silver surface texture finished with different treatments (Table 2). Sq parameter estimated globally in the entire sample and locally using a patch-based ensemble

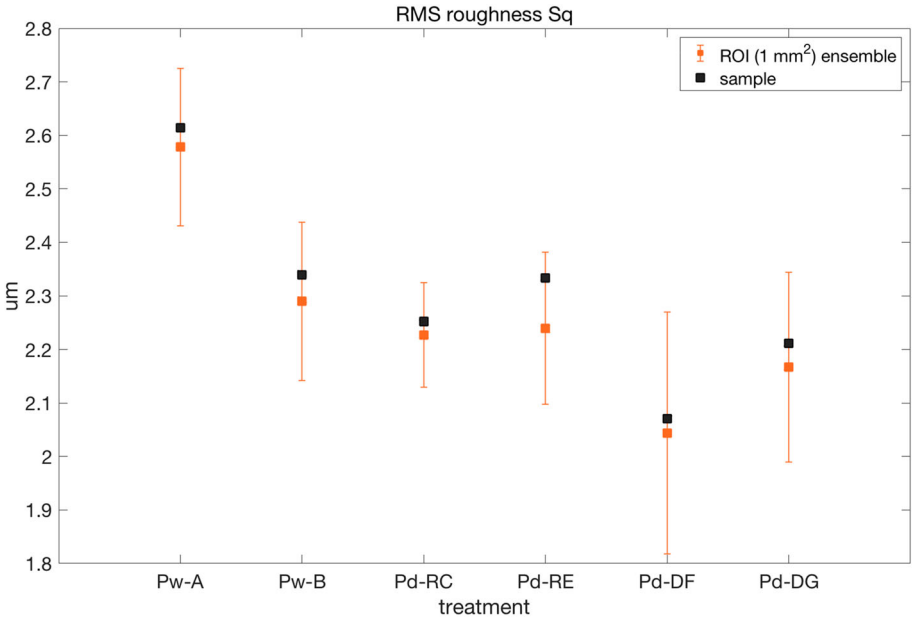

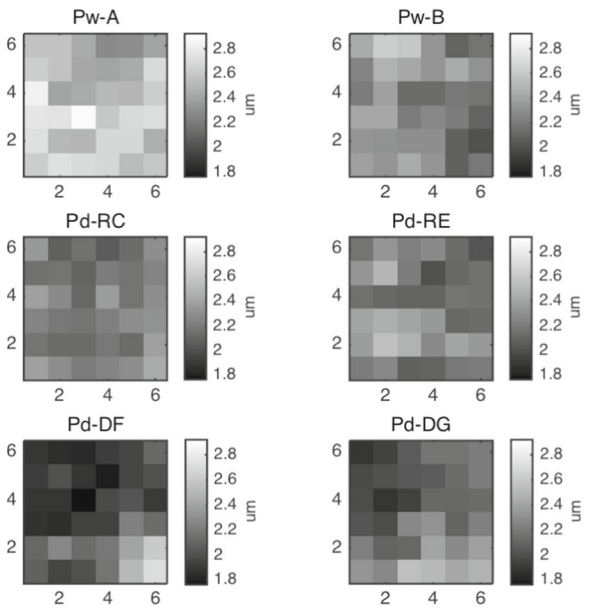

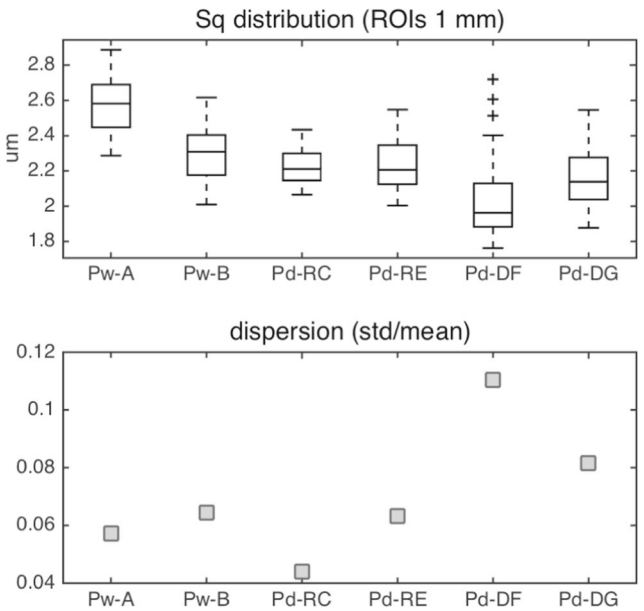

Fig. 8 Patch-based ensemble (1 mm^2 ROI): sample partitioning into local Sq roughness (left), boxplot and coefficient of variation of the Sq distribution (right)

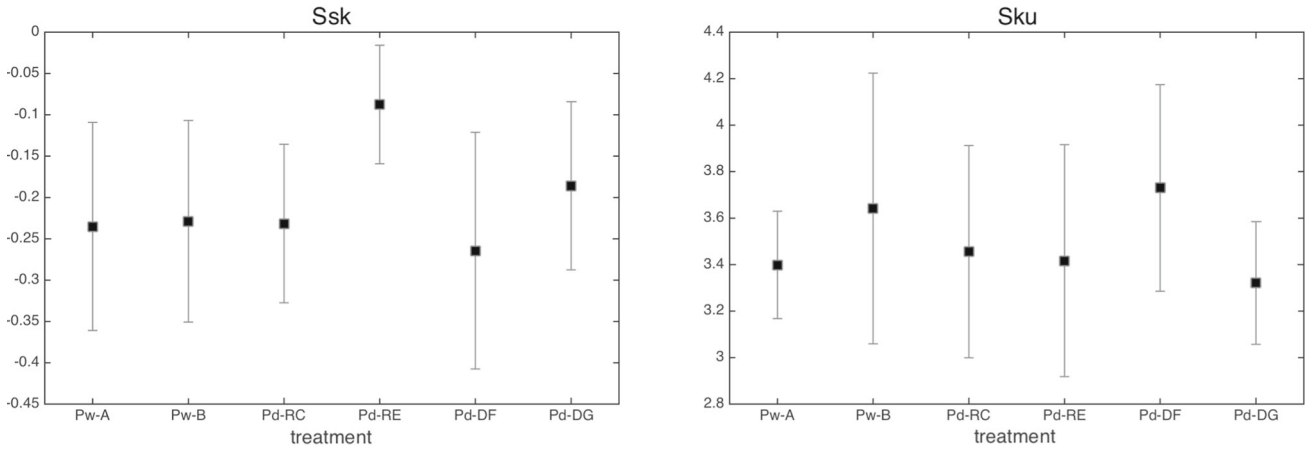

Fig. 9 Skewness and kurtosis of the surface computed locally using the patch-based ensemble (1 mm^2 ROI). Averaged value and standard deviation over the patches are given for each sample

The surface topography (see Fig. 3) is characterized by a succession of peaks and valleys due to the different treatments, with the amplitude density function (ADF) in the local ROI of nearly Gaussian characteristics. It is interesting to observe the behavior of the skewness and the kurtosis, estimated locally, by averaging over the ensemble (Fig. 9). Surface heights are approximately symmetrical about the mean plane, with small negative deviations of Ssk from the zero value, in fact, it is not observable a net predominance of peaks or valleys in the surface texture. Also the Sku values do not deviate significantly from the Normal distribution (threshold of 3). While recalling that the amplitude parameters do not carry univocal information regarding the shape of the topography, the kurtosis is in relation with the tail extremities of the ADF, for example due to peaks and valleys densely or sparsely distributed. High Sku values indicate the presence of outliers like scratches on the surface.

The nearly Gaussian surface roughness could be expected from the underlying abrasion process, however, putting in relation the Sq values with the characteristics of the abrasive medium observed at SEM is not generally possible as the artwork cleaning is carried out manually. The phenomena in surface processing at micron-scale, especially with the rubbers tools, are very complex, depending on parameters related both to the abrasive particles and the procedure; specific issues concerning tribology are far from the scope of this paper and specific literature is given [30–33].

Anyway, as shown above, the non-homogeneity of the surface roughness over the sample at the scale of interest can be inspected by looking at the distribution of the S-family parameters averaged in patch-based ROIs of suitable sizes. The 1 mm scale was retained interesting because it is visually perceivable and in the order of the size of the cleaning tools.

3.2 Signals separation

The other side of the multiscale analysis is the roughness and waviness separation, as follows from the flowchart in Fig. 5. The crucial point here is the choice of the cutoff scale to extract the two signals.

Figure 10 shows the variation of the roughness parameters for increasing cutoffs, from 50 μm to 1 μm. The statistics was computed on the high-frequency signal, obtained by Gaussian filtering.

It is evident the similar behavior of the Sq toward convergent values for the different treatments. It can be observed that the surface treated with the sodium bicarbonate powder of larger grain size (`Pw-A`) exhibits a greater Sq than the one polished with the rubber of fine grain size (`Pd-DF`, `Pd-DG`).

Also the Ssk and Sku scale-limited moments exhibit a similar behavior. From a statistical point of view, the treatments have the same nature of a low-abrasion process, but the mechanical action at microscopic level is different. In fact, the wet cleaning involves free abrasive particles suspended in liquid, while the dry cleaning involves abrasive grains bonded in elastic medium. The whole process, and hence the observed differences in the roughness in the scale-limited components, depends on both microscopic and macroscopic factors: from the kind of abrasive medium, the kind of treatment, to the manual procedure applied by the restorer that implies, for example, different pressures and path in which the tool is moved. It is expected that at the longer scales the contribution can be put in relation with the waviness induced by the process, while at the lower ones it should be put in relation with the abrasive medium. Looking at the multiscale statistics of Fig. 10 a two-phase behavior can be observed, suggesting to inspect the surface at the characteristic scale of $\sim$ 250 μm, or even at the individual scales at which a stationary point in Sku, for example, or in Sz, is found.

Following the above multiscale analysis, as exemplary result, in Fig. 11 is shown the three-dimensional topography map of the extracted roughness signal at the suggested cutoff of 250 μm, for the wet and dry treatments. The roughness amplitudes have similar statistics, but at this scale it can be observed the different textures generated by the wet abrasion (free particles) and the dry rubber (bonded grains). As depicted in Fig. 12, it is interesting to further study the surface components at the longer wavelengths with the

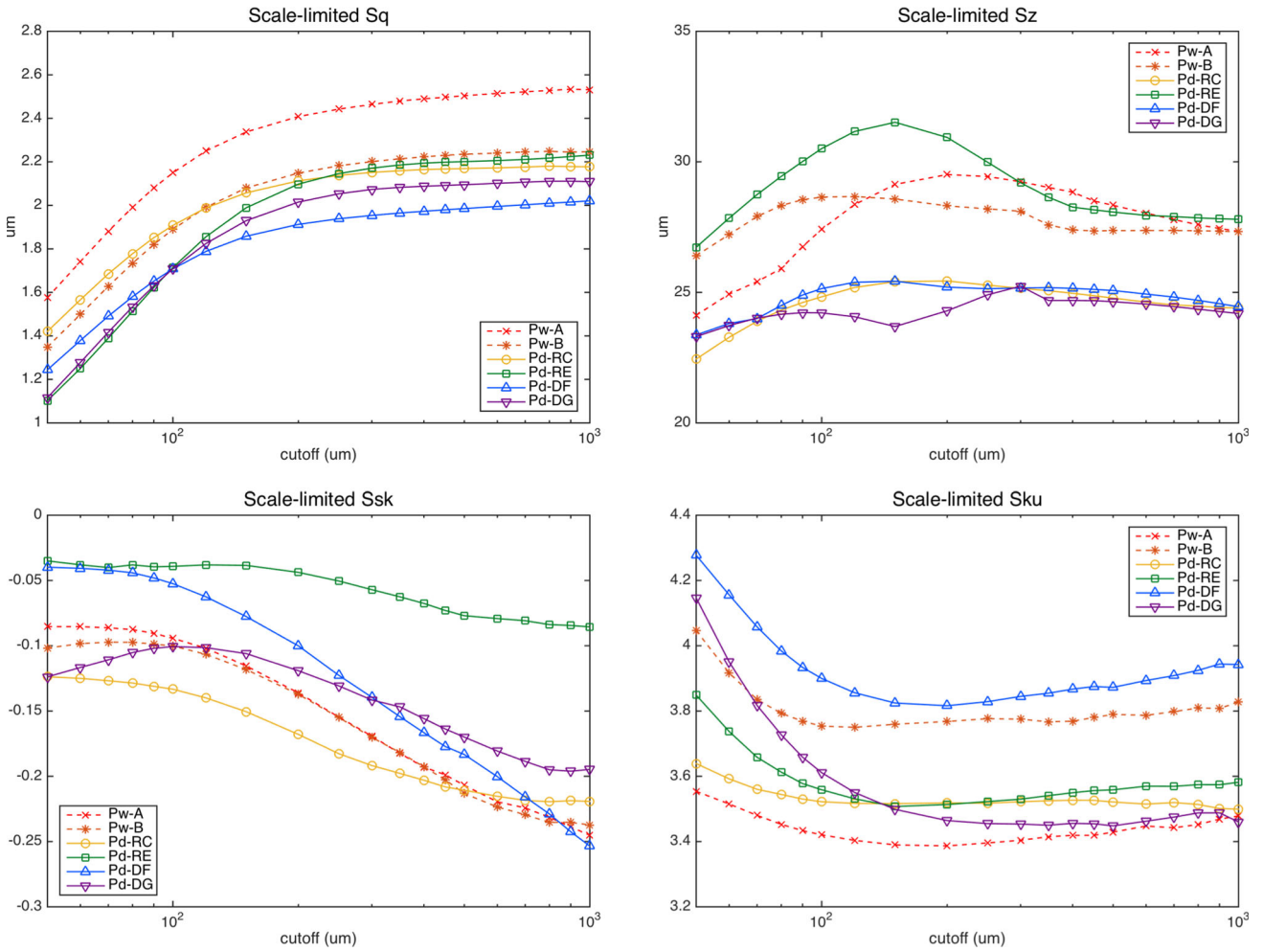

Fig. 10 Variation of the surface roughness parameters with the cutoff scale

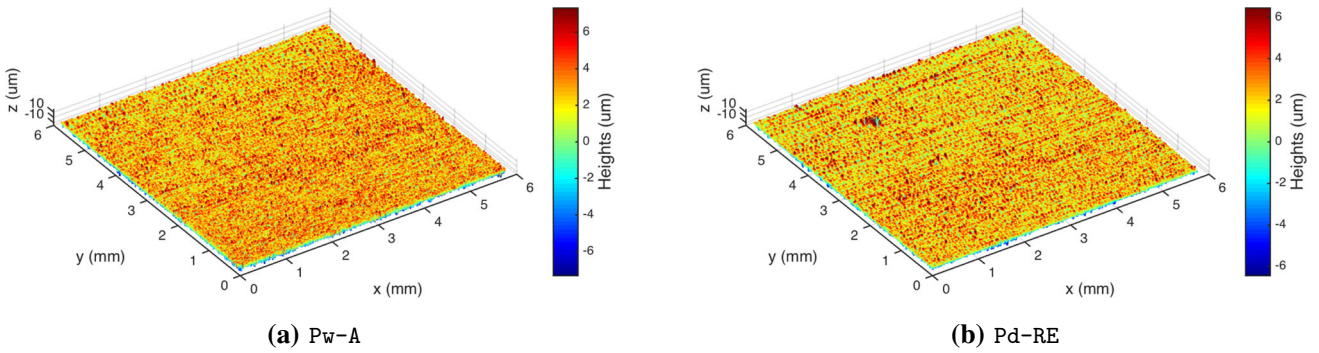

(a) `Pw-A` **(b)** `Pd-RE`

Fig. 11 Roughness signal (250 μm cutoff) of samples processed with wet (`Pw-A`) and dry treatment (`Pd-RE`)

aim of understanding the waviness signal left by the cleaning tool used. At the waviness scale, using a cutoff of 250 μm, 500 μm, and 1 mm, it is observable the crisscross pattern followed by the restorer in the treatment application, and the different sizes of the tools used. However, it is difficult to discriminate a well-defined fingerprint because the waviness pattern gathers the contributions of several effects such as, beside the pressure of the hand, the kind of tool or the deformation of the whole surface.

Finally, in Fig. 13 the position of the sample in the Ssk-Sku space is shown for the scale-limited surface with two cutoffs: the 1 mm cutoff and a sample-specific cutoff based on the minimum of the scale-limited Sku. It can be observed that the lower cutoff tends to cluster samples toward Gaussian threshold values, Ssk = 0 and Sku = 3, as expected at the scale where the signal related to the low-abrasion process dominates.

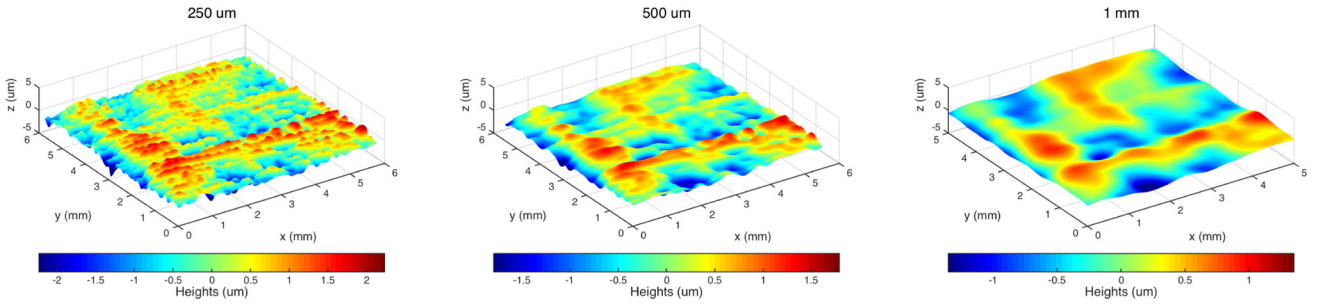

(a) Pw-A

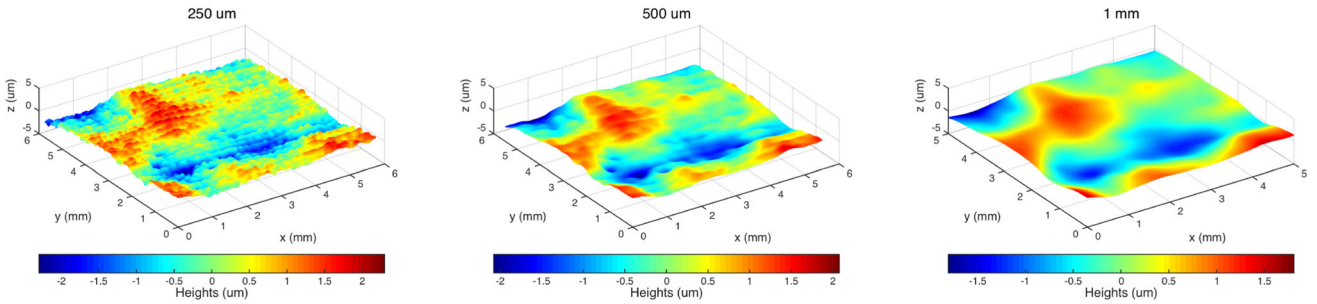

(b) Pd-RE

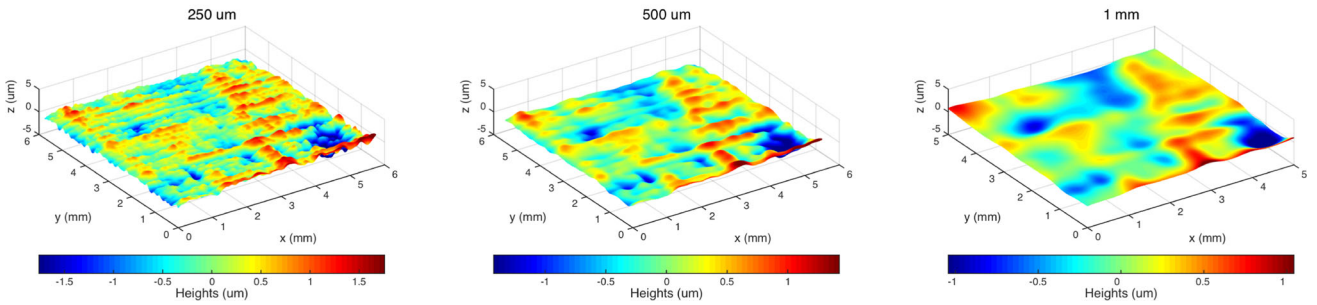

(c) Pd-DF

Fig. 12 Longer wavelengths decomposition at cutoff of 250 µm, 500 µm and 1000 µm of selected silver samples with different surface finishes: traditional cleaning (Pw-A) and dry cleaning with pencil (Pd-RE) and wheel (Pd-DF) tools

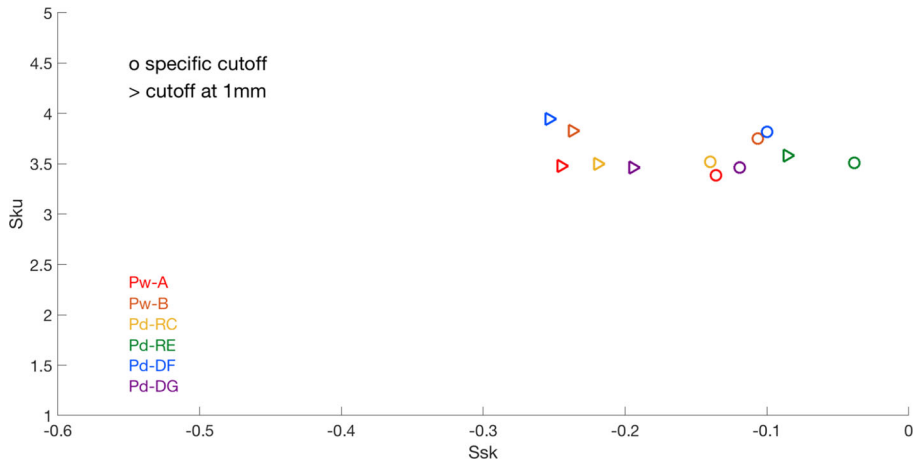

Fig. 13 Kurtosis (Sku) versus skewness (Ssk) for two selected cutoffs: 1 mm and a specific cutoff choice for each sample based on the minimum Sku values

4 Discussion and conclusions

In this research, we presented the application of the optical scanning profilometry based on conoscopic holography on the challenging measurement of the highly reflective surface of silver samples. The proof of concept on silver cleaning treatments allowed to demonstrate the effectiveness of this technique in the measurement of the shiny and smooth metal surface paving the way for in situ monitoring of real artworks. In fact, differently from the most of the commonly employed techniques, the proposed instrument has the possibility to measure macro-regions of the objects with micrometer resolution in depth (0.1 μm) and lateral (5 μm) directions. This enabled to evaluate the information conveyed from the surface from the low to the high spatial frequencies, including the waviness that needed such high depth accuracy as for roughness measurement, but larger dimensions for evaluating widely spaced variations. Moreover, the dense lateral sampling enabled the computation both of amplitude and hybrid areal roughness parameters. The experiment on silver treatments showed how the main structures of the surface were reliably represented in the bandwidth of the measurement, which was able to detect the relevant features characterizing the texture.

A novel, integrated multiscale roughness analysis was demonstrated for the examination of the hand-processed surfaces in artwork diagnostics. The proposed approach inspects the variation of the roughness features with the scale on two aspects: the evaluation length and the Gaussian cutoff.

The first analysis allowed to deal with possible non-homogeneity of the sample given that the treatment is carried out manually. In general, we showed how the computation of the S-family roughness parameters averaged in a patch-based ensemble of suitable size enables an effective analysis of the surface. Regarding the diagnostics, we found that the surfaces processed with the innovative dry treatments (rubbers) and the wet abrasive powders had similar Sq values and that the amplitude distributions, locally, were nearly Gaussian.

The second analysis showed a similar behavior of the roughness parameters with the cutoff scale for the different treatments, with the Sq parameter converging to stationary values. From a statistical point of view, the treatments have the same nature of the low-abrasion, but the mechanical process underlying wet and dry cleaning is different, thus leading to differences in the surface signal. The behavior of the multiscale S-family parameters suggested the scale at which to characterize the surface, with a choice of roughness cutoffs that can even be sample-specific. Regarding the waviness, a different topography was observed for the different cleaning tools, revealing the path and the size of the tools applied. Even if a well-defined fingerprint is difficult to extract in hand-made treatments, this interesting result opens to more general applications of surface metrology in heritage science.

Thus, the multiscale approach allowed a more accurate and meaningful analysis of the surface roughness both to monitor inhomogeneities and to understand the relevant scale of interest in signal separation, also in relation to the functional characterization of the surface process. If a high-resolution and high-accurate microsurface dataset is acquired, the method offers a novel tool for treatment monitoring in highly reflective metal artworks.

Acknowledgements This work was supported by the Scan4Reco project funded by EU Horizon 2020 Framework Programme for Research and Innovation under Grant Agreement No. 665091. The authors thank Vittorio Barra, formerly at University of Verona, for the visible-infrared technical photography. The samples were provided by Andrea Cagnini and Monica Galeotti from the Opificio delle Pietre Dure, Florence.

Data Availability Statement This manuscript has associated data in a data repository. [Authors' comment: Data are available from the corresponding author on reasonable request.]

A Statistical descriptors

"Appendix" summarizes the definitions of the parameters used. In each formula, A represents the sampling area and the function $z(x, y)$ the surface heights relative to the best fitting plane.

A.1 Amplitude parameters

A.1.1 Root mean square height (Sq)

$$Sq = \sqrt{\frac{1}{A}\int\int_A z^2(x, y)dxdy}. \tag{1}$$

A.1.2 Skewness (Ssk)

$$Ssk = \sqrt{\frac{1}{A}\frac{1}{Sq^3}\int\int_A z^3(x,y)dxdy}. \tag{2}$$

A.1.3 Kurtosis (Sku)

$$Sku = \sqrt{\frac{1}{A}\frac{1}{Sq^4}\int\int_A z^4(x,y)dxdy}. \tag{3}$$

A.1.4 Peak-to-valley roughness (Sz)

$$Sz = Sp + |Sv| \tag{4}$$

where Sp is the maximum peak height and Sv is the height of the lowest valley of the surface.

A.2 Hybrid parameters

A.2.1 RMS gradient (Sdq)

$$Sdq = \sqrt{\frac{1}{A}\int\int_A \left[\left(\frac{\partial z(x,y)}{\partial x}\right)^2 + \left(\frac{\partial z(x,y)}{\partial y}\right)^2\right]dxdy}. \tag{5}$$

A.2.2 Developed interfacial area ratio (Sdr)

$$Sdr = \frac{1}{A}\left[\int\int_A \left(\sqrt{1+\left(\frac{\partial z(x,y)}{\partial x}\right)^2 + \left(\frac{\partial z(x,y)}{\partial y}\right)^2} - 1\right)dxdy\right]. \tag{6}$$

References

1. J.P. Franey, G.W. Kammlott, T.E. Graedel, The corrosion of silver by atmospheric sulfurous gases. Corros. Sci. **25**(2), 133–143 (1985)
2. Michael B. Mcneil, Brenda J. Little, Corrosion mechanisms for copper and silver objects in near-surface environments. J. Am. Inst. Conserv. **31**(3), 355–366 (1992)
3. R.J.H. Wanhill, Brittle archaeological silver: a fracture mechanism and mechanics assessment. Archaeometry **45**(4), 625–636 (2003)
4. T. Palomar, B.R. Barat, E. García, E. Cano, A comparative study of cleaning methods for tarnished silver. J. Cult. Herit. **17**, 20–26 (2016)
5. T. Palomar, M. Oujja, I. Llorente, B.R. Barat, M.V. Cañamares, E. Cano, M. Castillejo, Evaluation of laser cleaning for the restoration of tarnished silver artifacts. Appl. Surf. Sci. **387**, 118–127 (2016)
6. G. Basilissi, A. Brini, A. Cagnini, C. Ortolani, A.S. Barbone, Evaluation of a dry method using erasers for silver–copper alloy tarnish cleaning and comparison with traditional methods. *J. Am. Inst. Conserv.*, pp. 1–17 (2021)
7. Pedro Gaspar, Charlotte Hubbard, David McPhail, Alan Cummings, A topographical assessment and comparison of conservation cleaning treatments. J. Cult. Herit. **4**, 294–302 (2003)
8. Jan Marczak, Andrzej Koss, Piotr Targowski, Michalina Góra, Marek Strzelec, Antoni Sarzyński, Wojciech Skrzeczanowski, Roman Ostrowski, Antoni Rycyk, Characterization of laser cleaning of artworks. Sensors **8**(10), 6507–6548 (2008)
9. C.S. Cheung, M. Spring, H. Liang, Ultra-high resolution Fourier domain optical coherence tomography for old master paintings. Opt. Express **23**(8), 10145–10157 (2015)
10. Tom Callewaert, Jerry Guo, Guusje Harteveld, Abbie Vandivere, Elmar Eisemann, Joris Dik, Jeroen Kalkman, Multi-scale optical coherence tomography imaging and visualization of Vermeer's girl with a pearl earring. Opt. Express **28**(18), 26239–26256 (2020)
11. M. Gómez-Heras, M.A. de Buergo, E. Rebollar, M. Oujja, M. Castillejo, R. Fort, Laser removal of water repellent treatments on limestone. Appl. Surf. Sci. **219**(3), 290–299 (2003)
12. C. Vazquez-Calvo, M.A. de Buergo, R. Fort, M.J. Varas-Muriel, The measurement of surface roughness to determine the suitability of different methods for stone cleaning. J. Geophys. Eng. **9**(4), S108–S117 (2012)

13. E.G. Ioanid, A. Ioanid, D.E. Rusu, F. Doroftei, Surface investigation of some medieval silver coins cleaned in high-frequency cold plasma. J. Cult. Herit. **12**(2), 220–226 (2011)
14. Pierluigi Carcagni, Claudia Daffara, Raffaella Fontana, Maria Chiara Gambino, Maria Mastroianni, Cinzia Mazzotta, Enrico Pampaloni, and Luca Pezzati. Optical micro-profilometry for archaeology. Proc. SPIE **5857**, 58570F (2005)
15. Gabriel Y. Sirat, Conoscopic holography i basic principles and physical basis. J. Opt. Soc. Am. A **9**(1), 70 (1992)
16. Y. Malet, G.Y. Sirat, Conoscopic holography application: multipurpose rangefinders. J. Opt. **29**(3), 183–187 (1998)
17. G.S. Spagnolo, R. Majo, M. Carli, D. Ambrosini, D. Paoletti, Virtual gallery of ancient coins through conoscopic holography. Proc. SPIE **5146**, 202–209 (2003)
18. J. Striova, R. Fontana, M. Barucci, A. Felici, E. Marconi, E. Pampaloni, M. Raffaelli, C. Riminesi, Optical devices provide unprecedented insights into the laser cleaning of calcium oxalate layers. Microchem. J. **124**, 331–337 (2016)
19. Alice Dal Fovo, George J. Tserevelakis, Evgenia Klironomou, Giannis Zacharakis, Raffaella Fontana, First combined application of photoacoustic and optical techniques to the study of an historical oil painting. Eur. Phys. J. Plus **136**, 757 (2021)
20. S. Mazzocato, C. Daffara, Experiencing the untouchable: a method for scientific exploration and haptic fruition of artworks microsurface based on optical scanning profilometry. *Sensors*, 21(13), (2021).
21. Nicola Gaburro, Giacomo Marchioro, Claudia Daffara, A versatile optical profilometer based on conoscopic holography sensors for acquisition of specular and diffusive surfaces in artworks. Proc. SPIE **10331**, 48–56 (2017)
22. Wantao He, Kai Zhong, Zhongwei Li, Xu. Xianglin Meng, Xingjian Liu Cheng, Yusheng Shi, Accurate calibration method for blade 3d shape metrology system integrated by fringe projection profilometry and conoscopic holography. Opt. Lasers Eng. **110**, 253–261 (2018)
23. D.J. Whitehouse, *Handbook of Surface Metrology* (Institute of Physics Publishing, Bristol, 1994)
24. Maxence Bigerelle, Thomas Mathia, Salima Bouvier, The multi-scale roughness analyses and modeling of abrasion with the grit size effect on ground surfaces. Wear **286–287**, 124–135 (2012)
25. Gaëtan. Le Goïc, Maxence Bigerelle, Serge Samper, Hugues Favrelière, Maurice Pillet, Multiscale roughness analysis of engineering surfaces: A comparison of methods for the investigation of functional correlations. Mech. Syst. Signal Process. **66–67**, 437–457 (2016)
26. C. Daffara, N. Gaburro, G. Marchioro, A. Romeo, G. Basilissi, A. Cagnini, M. Galeotti, Surface micro-profilometry for the assessment of the effects of traditional and innovative cleaning treatments of silver, in *Lasers in the Conservation of Artworks XI*. ed. by P. Targowski. et al. Proceedings of LACONA XI. (NCU Press, Torun, Poland, 2017), pp. 127–140
27. ISO 25178-2. Geometrical Product Specifications (GPS) - surface texture: Areal - part 2: Terms, definitions and surface texture parameters. Technical report, International Organization for Standardization, (2012).
28. R. Leach (ed.), *Characterisation of Areal Surface Texture* (Springer, Heidelberg, 2013)
29. Árpád Czifra, István Barányi. Sdq-sdr topological map of surface topographies. *Frontiers in Mechanical Engineering*, 6, (2020)
30. B. Bhushan, *Surface Roughness Analysis and Measurement Techniques in Modern Tribology Handbook* (CRC Press, Boca Raton, 2001)
31. J.J. Coronado, Effect of abrasive size on wear. In *Abrasion Resistance of Materials*. InTech, (2012).
32. Y.P. Wu, Y. Zhou, J.L. Li, H.D. Zhou, J.M. Chen, H.C. Zhao, A comparative study on wear behavior and mechanism of styrene butadiene rubber under dry and wet conditions. Wear **356–357**, 1–8 (2016)
33. T.A.M. Counsell, J.M. Allwood, Using abrasives to remove a toner-print so that office paper might be reused. Wear **266**(7–8), 782–794 (2009)